

Chemical Control of Interstitial Iron Leading to Superconductivity in $\text{Fe}_{1+x}\text{Te}_{0.7}\text{Se}_{0.3}$

Efrain E. Rodriguez^a, Christopher Stock^{a,b}, Ping-Yen Hsieh^{a,c}, Nicholas Butch^d, Johnpierre Paglione^d and Mark A. Green^{a,c,*}

^a NIST Center for Neutron Research, NIST, Gaithersburg, MD 20899 USA; E-mail: mark.green@nist.gov

^b Indiana University, 2401 Milo B. Sampson Lane, Bloomington, Indiana 47408 USA

^c Department of Materials Science and Engineering, University of Maryland, College Park, 20742 USA

^d Center for Nanophysics and Advanced Materials, University of Maryland, College Park, MD 20742 USA

Supplementary Information

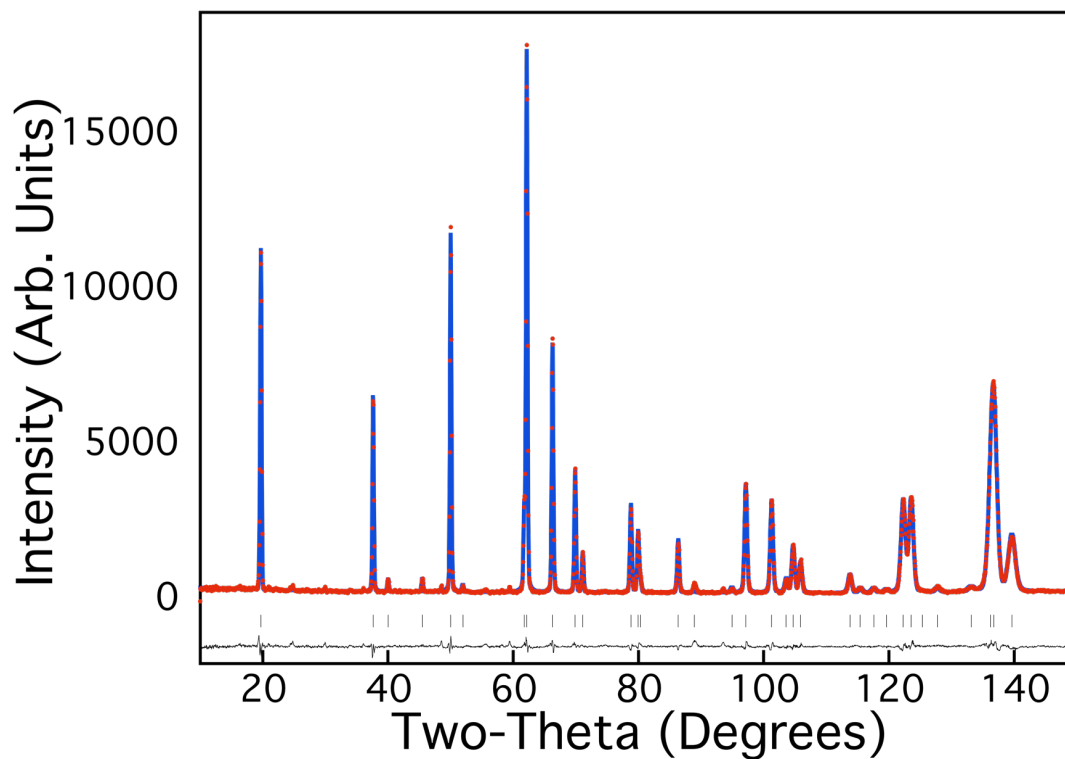


Figure S1 Observed, calculated and difference obtained from Rietveld refinements of powder neutron diffraction data of $\text{Fe}_{1.048(2)}\text{Te}_{0.7}\text{Se}_{0.3}$ at 7 K using the Ge311 monochromator.

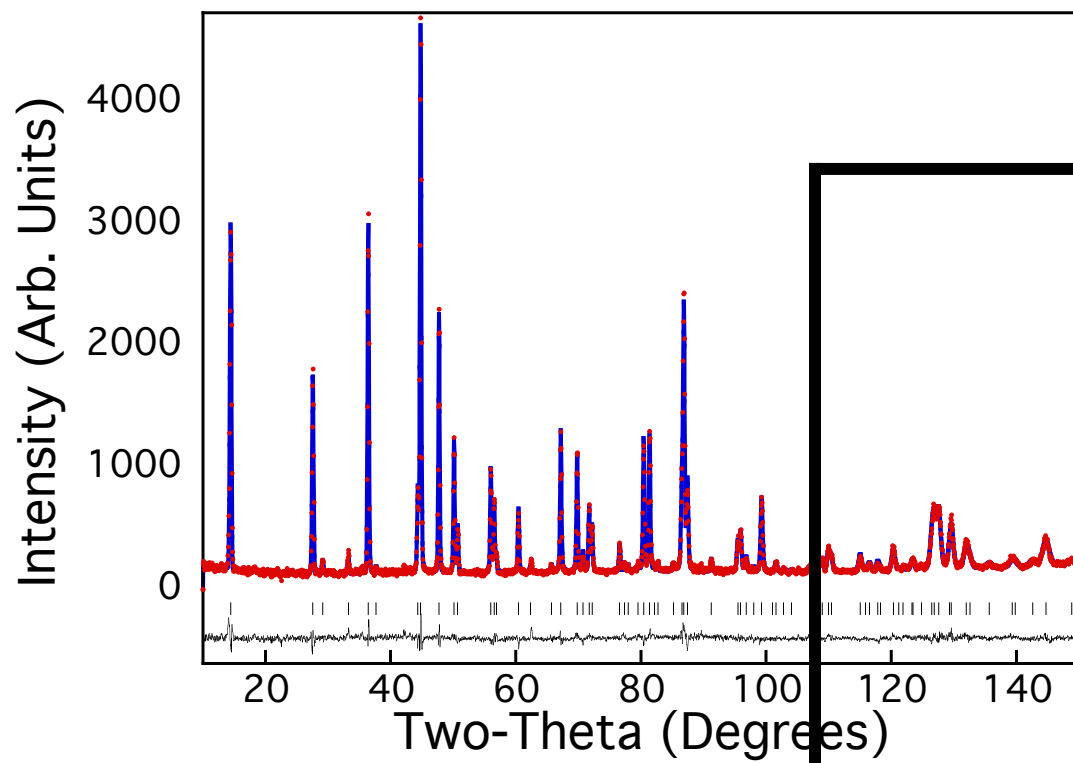


Figure S2 Observed, calculated and difference obtained from Rietveld refinements of powder neutron diffraction data of $\text{Fe}_{1.048(2)}\text{Te}_{0.7}\text{Se}_{0.3}$ at 7 K using the Cu311 monochromator.

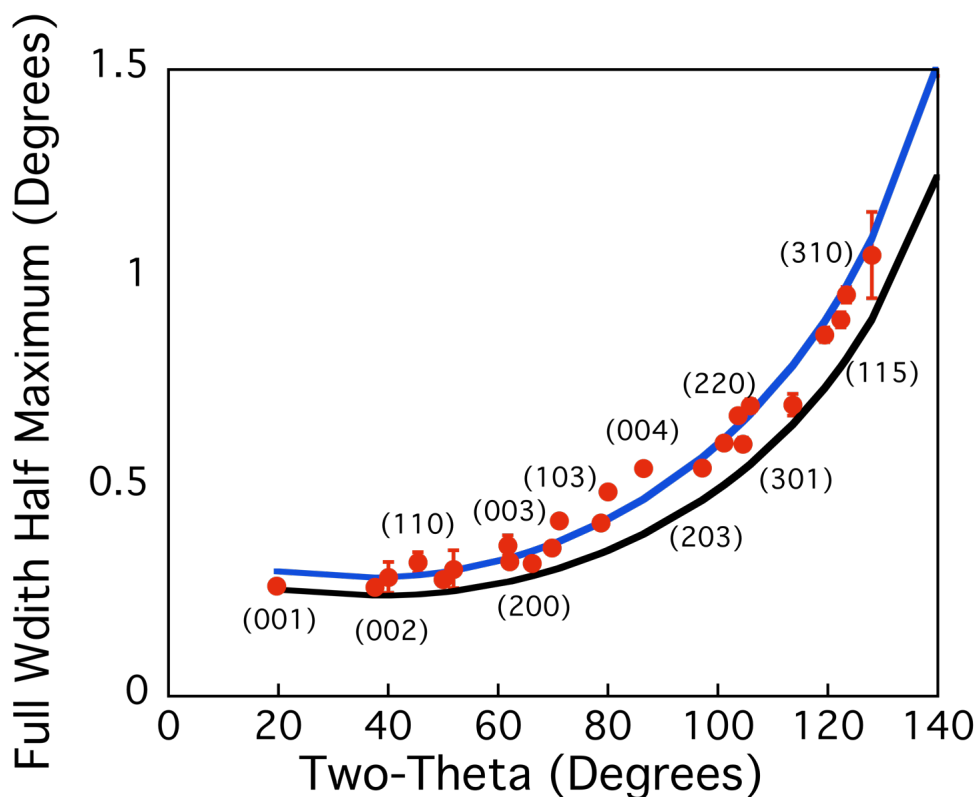


Figure S3 Full width at half maximum of a selection of the Bragg reflections for $\text{Fe}_{1.009(3)}\text{Te}_{0.7}\text{Se}_{0.3}$ at 7K; the data that shows the greatest amount of isotropic gaussian strain. The black curve represents a typical resolution curve for the BT1 powder neutron diffractometer. The increased peak shape broadening, represented by the blue curve for this materials, is well fitted to an isotropic strain parameter. This gaussian term with a $\tan^2\theta$ dependence was employed to account for peak broadening that varies across the series as well as with temperature. An orthorhombic strain on a tetragonal lattice model did not improve the fit the broadening is not restricted or larger in the ab plane. For example, the (110) and (220) are broadened with respect to the resolution curve, that would possibly imply an orthorhombic strain. However, the (003) and (004) also broaden significantly with temperature, whereas the (200) does not, which is not consistent with orthorhombic strain. The temperature below which this strain occurs at ~ 200 K is also inconsistent with the temperature (< 70 K) that FeSe and Fe_{1+x}Te become orthorhombic. This confirms that the strain is a result of structural origin such as misfitting layers or as a result of the very different Fe- Te and Fe - Se bond distances or a slight distortion to a symmetry lower than orthorhombic.

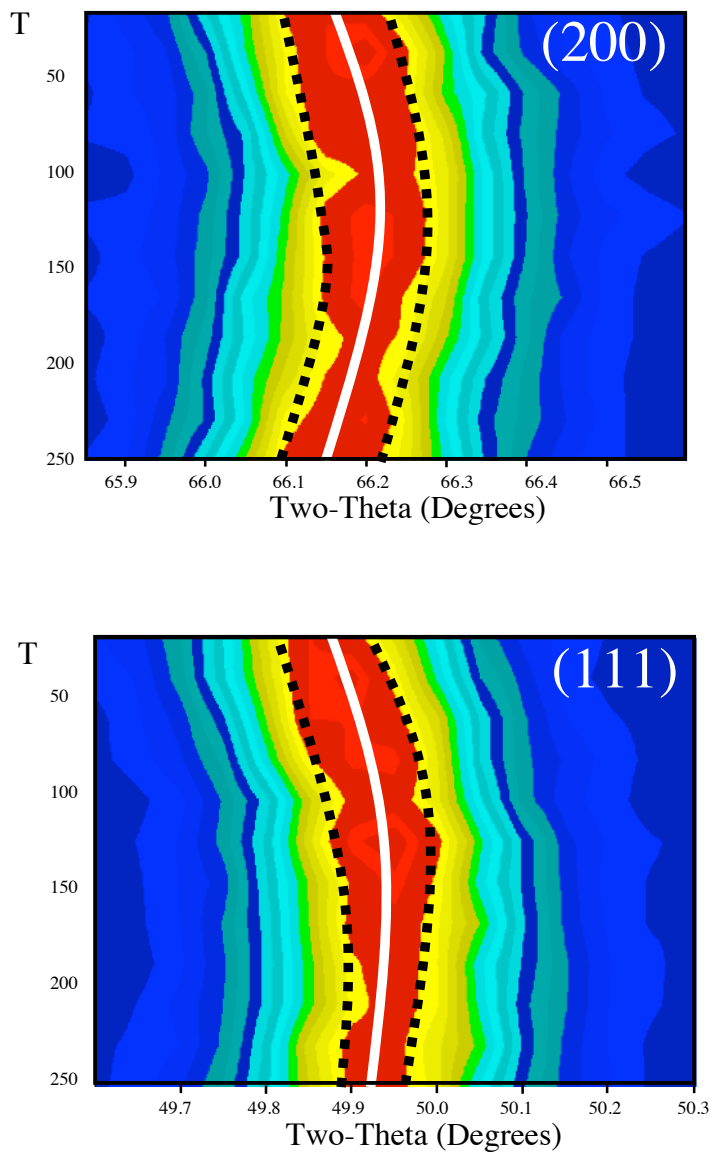
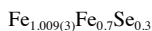
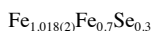


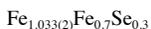
Figure S4 Position of the (200) and (111) reflection as a function of temperature, highlighting the negative and then positive variation of lattice parameters on cooling from 250 K to base, which is associated with a slight broadening of the reflection at low temperature as a result of the strain within the lattice. The (111) is much less pronounced than the (200) as a result of the c component.



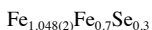
Temperature	T_{e_z}	Se_z	a (Å)	c (Å)	R_p, χ^2
20 K	0.2147 (9)	0.270 (2)	3.80368 (5)	6.0696 (2)	9.54, 1.26
30 K	0.214 (1)	0.267 (2)	3.80343 (5)	6.0703 (2)	10.0, 1.32
40 K	0.2148 (9)	0.270 (2)	3.80298 (5)	6.0723 (1)	10.2, 1.32
60 K	0.2140 (9)	0.270 (2)	3.80238 (5)	6.0751 (1)	9.73, 1.26
80 K	0.2155 (9)	0.272 (2)	3.80209 (5)	6.0784 (1)	9.54, 1.23
100 K	0.2157 (9)	0.270 (2)	3.80194 (5)	6.0831 (1)	9.43, 1.22
125 K	0.2136 (9)	0.272 (2)	3.80146 (5)	6.0874 (1)	9.54, 1.30
150 K	0.2147 (9)	0.274 (2)	3.80166 (5)	6.0928 (1)	10.0, 1.26
175 K	0.2164 (9)	0.271 (2)	3.80181 (5)	6.0973 (1)	9.47, 1.27
200 K	0.217 (1)	0.274 (2)	3.80227 (5)	6.1021 (2)	9.60, 1.35
225 K	0.214 (1)	0.275 (2)	3.80330 (6)	6.1088 (2)	9.34, 1.29
250 K	0.217 (1)	0.275 (2)	3.80390 (6)	6.1117 (2)	9.85, 1.42
275 K	0.218 (1)	0.278 (2)	3.80536 (7)	6.1171 (2)	9.90, 1.45



Temperature	T_{e_z}	Se_z	$Fe2_z$	a (Å)	c (Å)	R_p, χ^2
20 K	0.215 (1)	0.262 (3)	0.74 (3)	3.80109 (7)	6.0706 (2)	6.61, 0.91
30 K	0.213 (1)	0.257 (2)	0.72 (2)	3.80080 (7)	6.0713 (2)	6.90, 0.91
40 K	0.213 (1)	0.258 (2)	0.72 (3)	3.80082 (7)	6.0726 (2)	6.28, 0.87
60 K	0.212 (1)	0.261 (2)	0.71 (2)	3.80013 (6)	6.0751 (2)	6.39, 0.88
80 K	0.213 (1)	0.259 (2)	0.71 (2)	3.79955 (7)	6.0781 (2)	6.48, 0.87
100 K	0.213 (1)	0.262 (2)	0.69 (2)	3.79967 (6)	6.0815 (2)	6.64, 0.83
120 K	0.212 (1)	0.256 (2)	0.68 (2)	3.79947 (6)	6.0848 (2)	6.91, 0.88
140 K	0.211 (1)	0.262 (3)	0.71 (3)	3.79974 (7)	6.0894 (2)	6.62, 0.83
160 K	0.213 (1)	0.260 (3)	0.71 (3)	3.79970 (7)	6.0929 (2)	6.73, 0.89
180 K	0.215 (1)	0.258 (3)	0.69 (2)	3.80007 (7)	6.0966 (2)	6.85, 0.93
200 K	0.212 (1)	0.260 (2)	0.69 (2)	3.80040 (7)	6.1007 (2)	6.80, 0.90
225 K	0.212 (1)	0.260 (3)	0.71 (3)	3.80155 (7)	6.1053 (2)	6.84, 0.91
250 K	0.211 (1)	0.259 (2)	0.69 (2)	3.80242 (7)	6.1106 (2)	6.73, 0.86
275 K	0.212 (2)	0.261 (3)	0.72 (4)	3.80372 (9)	6.1136 (2)	8.10, 0.92



Temperature	T_{e_z}	Se_z	$Fe2_z$	a (Å)	c (Å)	R_p, χ^2
20 K	0.212 (1)	0.261 (2)	0.79 (1)	3.80168 (6)	6.0726 (1)	8.04, 0.86
30 K	0.211 (1)	0.258 (2)	0.72 (1)	3.80125 (6)	6.0730 (2)	7.59, 0.92
40 K	0.211 (1)	0.262 (2)	0.75 (1)	3.80107 (6)	6.0741 (2)	7.95, 0.84
60 K	0.211 (1)	0.263 (2)	0.78 (1)	3.80063 (6)	6.0767 (1)	7.94, 0.89
80 K	0.209 (1)	0.258 (2)	0.74 (1)	3.80036 (6)	6.0790 (1)	8.64, 0.86
120 K	0.208 (1)	0.262 (2)	0.78 (1)	3.79989 (6)	6.0864 (1)	7.55, 0.81
160 K	0.209 (1)	0.263 (2)	0.75 (2)	3.80042 (6)	6.0934 (2)	7.97, 0.9
200 K	0.208 (1)	0.261 (2)	0.73 (1)	3.80129 (6)	6.1012 (2)	7.86, 0.79
250 K	0.212 (1)	0.267 (3)	0.76 (2)	3.80313 (7)	6.1097 (2)	8.48, 0.83



Temperature	T_{e_z}	Se_z	$Fe2_z$	a (Å)	c (Å)	R_p, χ^2
20 K	0.2097 (6)	0.261 (1)	0.777 (5)	3.80088 (4)	6.07397 (8)	7.09, 0.90
40 K	0.2100 (6)	0.261 (1)	0.770 (5)	3.80045 (4)	6.07483 (8)	7.02, 0.86
60 K	0.2100 (6)	0.262 (1)	0.771 (5)	3.79999 (4)	6.07717 (8)	7.21, 0.89
80 K	0.2112 (7)	0.262 (1)	0.780 (5)	3.79948 (4)	6.07960 (8)	7.31, 0.95
120 K	0.2103 (7)	0.262 (1)	0.777 (6)	3.79925 (4)	6.08666 (8)	7.45, 0.92
140 K	0.2089 (7)	0.262 (1)	0.775 (6)	3.79948 (4)	6.09054 (9)	7.21, 0.91
180 K	0.2101 (7)	0.260 (1)	0.783 (6)	3.79990 (4)	6.09741 (9)	7.78, 0.97
220 K	0.2102 (7)	0.262 (1)	0.792 (6)	3.80131 (4)	6.10544 (9)	7.25, 0.91
260 K	0.2087 (8)	0.258 (1)	0.758 (6)	3.80269 (5)	6.1103 (1)	8.34, 1.06

Table S1 Structural parameters for $\text{Fe}_{1.009(3)}\text{Fe}_{0.7}\text{Se}_{0.3}$, $\text{Fe}_{1.018(2)}\text{Fe}_{0.7}\text{Se}_{0.3}$, $\text{Fe}_{1.033(2)}\text{Fe}_{0.7}\text{Se}_{0.3}$, and $\text{Fe}_{1.048(2)}\text{Fe}_{0.7}\text{Se}_{0.3}$ as a function of temperature. The position of the interstitial iron for $\text{Fe}_{1.009(3)}\text{Fe}_{0.7}\text{Se}_{0.3}$ was not stable in these very short scans at $\lambda = 2.0787$ Å.